Sustainable cooling strategies to reduce tool wear, power consumption and surface roughness during ultrasonic assisted turning of Ti-6Al-4V

Jay Airao [a], Chandrakant K. Nirala [a], Rachele Bertolini [b], Grzegorz M. Krolczyk [c,*], Navneet Khanna [d,*]

[a] Department of Mechanical Engineering, Indian Institute of Technology Ropar, Rupnagar 140001, India
[b] Department of Industrial Engineering, University of Padova, Via Venezia 1, 35131 Padova, Italy
[c] Department of Manufacturing Engineering and Automation Products, Opole University of Technology, 76 Proszkowska St, 45-758 Opole, Poland
[d] Advanced Manufacturing Laboratory, Institute of Infrastructure Technology Research and Management (IITRAM), Ahmedabad 380026, India

ARTICLE INFO

ABSTRACT

Issues related to the machinability of difficult-to-machine materials such as Titanium and Nickel base superalloys are well explicated in the literature. In this regard, a novel study, applying ultrasonic vibration along with MQL and LCO_2, is proposed to enhance the machinability of Ti-6Al-4V. In this regard, this article attempts to analyze machinability of Ti-6Al-4V in conventional and Ultrasonic Assisted Turning (UAT) under dry, wet, MQL and LCO_2. The experiments are performed on an in-house developed ultrasonic assisted turning setup, keeping all the machining parameters constant. The main tool wear mechanisms observed are diffusion, adhesion, abrasion, and built-up edge formation in both cutting strategies. Moreover, the LCO_2 and ultrasonic vibration significantly reduce specific cutting energy without compromising the surface roughness and tool life. Ultimately, the LCO_2, along with ultrasonic assisted turning, promotes sustainability in the machining of Ti-6Al-4V.

1. Introduction

Titanium alloys are being used in biomedical, marine, aerospace, and automotive sectors owing to their admirable mechanical properties such as high specific strength, superior fatigue and creep resistance at elevated temperature, and good corrosion resistance [1]. However, some properties such as low thermal conductivity, chemical affinity, work hardening at elevated temperature, etc., make them difficult-to-cut materials. The poor machinability of Titanium alloys leads to reduce tool life and surface quality, raises the forces and power consumption, degrades the life of components, etc. [2]. Several alterations have been integrated to the existing machining techniques to enhance the machinability of those alloys. Some of them are ultrasonic-assisted turning (UAT) [3], laser-assisted machining [4], high-pressure jet-assisted machining [5], etc.

Ultrasonic assisted turning (UAT) is a hybrid machining technique where a frequency above 20 kHz is imposed on the cutting tool in the machining process. In the UAT, high resonance frequency and low amplitude are generally used for higher material removal rate (MRR). Ultrasonic vibration can be applied to the different machining processes such as grinding, drilling, turning and milling. Ultrasonic assisted machining has shown various advantages in the machining of difficult-to-machine materials. Bai et al. [6] executed the UAT of Inconel 718 and 625 to study the machining force and surface topography. It was observed that the UAT significantly improves surface topography and reduces cutting forces compared to conventional turning (CT) process. Zhang et al. [7] used elliptical vibration cutting to evaluate the tool wear behavior in the machining of 7050-T7451 aluminum alloy. They noted that the elliptical vibration reduces oxidation, adhesion and abrasion wear of the tool. Moreover, it also improves the surface quality. In a similar study, Lotfi et al. [8] employed 3D elliptical vibration in the machining of Ti-6Al-4V and analyzed that the 3D UAT reduces the cutting force and grain size approximately by 20–30% and 5%, respectively than CT. Likewise, in an ultrasonic-assisted diamond turning of FeCrCoMnNi, it was realized that the ultrasonic vibration generates a nanoscale burnishing effect on the machined surface that eliminates scratch formation and improves the surface quality [9]. In a recent study, Peng et al. [10] proposed high-speed UAT (HUAT) by applying the vibration in a radial direction in the machining of hardened steel. They reported 80% reduction in force and 1.5 times enhancement in tool life in HUAT compared to CT. Apart from turning, ultrasonic vibration is

* Corresponding authors.
  E-mail addresses: g.krolczyk@po.opole.pl (G.M. Krolczyk), navneetkhanna@iitram.ac.in (N. Khanna).

Nomenclature		V	Cutting speed (m/min)
		V_{cr}	Critical cutting speed (m/min)
a	Amplitude (µm)	R_a	Average surface roughness (µm)
a_p	Depth of cut (mm)	CT	Conventional turning
l	Length of horn (mm)	LN_2	Liquid nitrogen
ω_n	natural frequency of vibration (rad/s)	VB	Average width of flank wear (mm)
f	Feed (mm/rev)	BUE	Built-up edge
C	Speed of sound through solid (m/s)	LCO_2	Liquid carbon dioxide
F	Frequency (Hz)	MQL	Minimum quantity lubrication
P_I	Ideal power (W)	MRR	Material removal rate (mm^3/s)
P_M	Power consumed during machining (W)	SCE	Specific cutting energy (J/mm^3)
P_T	Total power (W)	UAT	Ultrasonic assisted turning

also implemented in milling and drilling processes. Ni et al. [11] carried out ultrasonic-assisted milling (UAM) of Titanium 64 to study the tool wear, machining forces and surface quality. It was concluded that the UAM lowers pulse cutting forces and catastrophic tool wear than in conventional milling. In a similar study of UAM on Ti-6Al-4V, Gao et al. [12] investigated that uniform surface topography in UAM was due to heat generation and chip adherence to the cutter, improving the quality of a machined surface. Sanda et al. [13] carried out ultrasonic-assisted drilling of Titanium 64 to the effect of ultrasonic vibration on surface roughness, force and hole quality. They found that thrust force and cutting temperature reduced significantly upon applying vibration, whereas burr formation was not much affected by vibrations. In a study on ultrasonic peening drilling of Ti-6Al-4V, Liu et al. [14] investigated that the surface roughness decreased by 37–69%, circumferential residual stresses increased by 225% and hole diameter accuracy increased by 33–69%.

Apart from the assisted techniques, the cutting fluids used in machining are also essential to enhance the machinability of the materials. Since the heat produced in machining of Titanium and Nickel base superalloy plays a vital role in machinability and tool wear, it is essential to decrease the heat from the cutting zone [15]. Different types of cooling strategies such as conventional flood cooling, MQL (minimum quantity lubrication), cryogenic cooling, liquid carbon dioxide (LCO_2) base cooling, cryo-MQL, etc., are being used in machining operations [16]. Conventional flood cooling uses synthetic-oil-based emulsion, which is not considered as sustainable, as it generates environmental disputes and is hazardous for human health. Concerning this, MQL, cryogenic cooling, LCO_2, and vegetable oil-based coolant have been evolving as sustainable cutting fluids. These cutting fluids minimize the issues that occur when conventional flood cooling is used [2]. In the MQL, oil particles are delivered in the form of mist to the machining zone, decreasing the friction at the interface zone. In cryogenic cooling, liquid nitrogen (LN_2) is provided to the cutting area, decreasing the heat from shear zones. The LCO_2 acts similarly as LN_2 due to its low boiling point temperature.

Over the decade, many researchers have used the above-mentioned cooling strategies during machining to make the process more efficient and sustainable. Khanna et al. [17] performed machining under dry, wet, MQL and CO_2 to compare the effect of various cooling strategies on the machinability of 15–5 PH stainless steel. The CO_2 reduced tool wear substantially compared to wet and MQL cooling, respectively. It also presented lower surface roughness and micro hardness values than dry, flood and MQL conditions. A similar study was performed on Ni-based superalloy 625 using MQL, cryogenic cooling (LN_2) and cryoMQL by Yildirim et al. [18]. Cryo MQL lowered surface roughness, cutting temperature and increased the tool life compared to cryogenic and MQL conditions. The tool wear mechanism detected were adhesion, abrasion and BUE formation under all the cooling conditions. Gajarani [19] executed a similar study on titanium 64 and noted that cryo MQL showed more reduction cutting and feed forces, surface roughness and

contact length than cryogenic and dry conditions. It was attributed to the simultaneous effect of cooling provided by LN_2 and aerosol in cryoMQL, enhancing the heat dissipation from the cutting zone. Chetan et al. [20] compared the machinability of titanium 64 under dry, wet and cryogenic cooling conditions. The cryogenic cooling reduced diffusion and adhesion, and improved tool life by 200% and 80% compared to dry and wet conditions. It was attributed to a lessening in heat at the cutting zone and thermal damage of the cutting tool, increasing the tool life and surface finish [21]. Similarly, Khanna et al. [22] did the comparative study on titanium 64 under MQL, wet and LCO_2 conditions and, observed that the cutting force and tool wear were higher under MQL than wet and LCO_2. The pressurized jet of LCO_2 reduced the friction and decreased the temperature, reducing the tool wear. The machinability of Ti-5553 under dry, LN_2 and LCO_2 conditions was analyzed by Kaynak and Gharibi [23]. It was noted that the plastic deformation on the rake face was dominant under LN_2 and adhesion and diffusion were dominant under LCO_2 and dry condition. Similar observations were made during milling of titanium 64 under dry, LN_2, CO_2 snow and MQL conditions by Jamil et al. [24]. Moreover, it was concluded that CO_2 snow outpaced in terms of tool wear, surface quality and carbon emission than LN_2, MQL and dry conditions.

From the above literature, it can be said that the UAT is a promising technique to enhance the machinability of titanium alloys. Additionally, it can also be said that the MQL and LCO_2 are better than dry and wet conditions and capable of providing a sustainable clarification for machining difficult-to-cut materials. Very few studies are found combining the effect of ultrasonic vibration and cryogenic cooling in machining super alloy [25]. Moreover, Agrawal et al. [26] combined the UAT with LN_2 and MQL in machining of Ti-6Al-4V. However, no study is known describing the machining performance using ultrasonic vibration and under MQL and LCO_2 for Ti-6Al-4V. Considering this, the following research gaps are identified; (1) Analysis of tool wear behavior in the UAT under dry, wet, MQL and LCO_2 (2) effect of tool wear on the surface roughness, power consumption and specific cutting energy of Ti-6Al-4V in UAT under dry, wet, MQL and LCO_2 and (3) Comprehensive and comparative analysis of tool wear and machinability of Ti-6Al-4V for CT and UAT under different cooling strategies. In this regard, the experiments are performed for CT and UAT under dry, wet, MQL and LCO_2 using Ti-6Al-4V as workpiece material. The outcomes in terms of tool wear, surface roughness, power consumption, specific cutting energy and chip morphology are examined.

2. Experimental procedure

As shown in Fig. 1, an in-house developed UAT setup is used to execute the experiments. The setup comprises a frequency generator, piezoelectric transducers, a horn, and a fixture. A fixture is assembled to the conventional lathe, as shown in Fig. 1. The frequency generator produces a high-frequency low voltage signal. This signal is supplied to the piezoelectric transducer attached at the top end of the horn. The
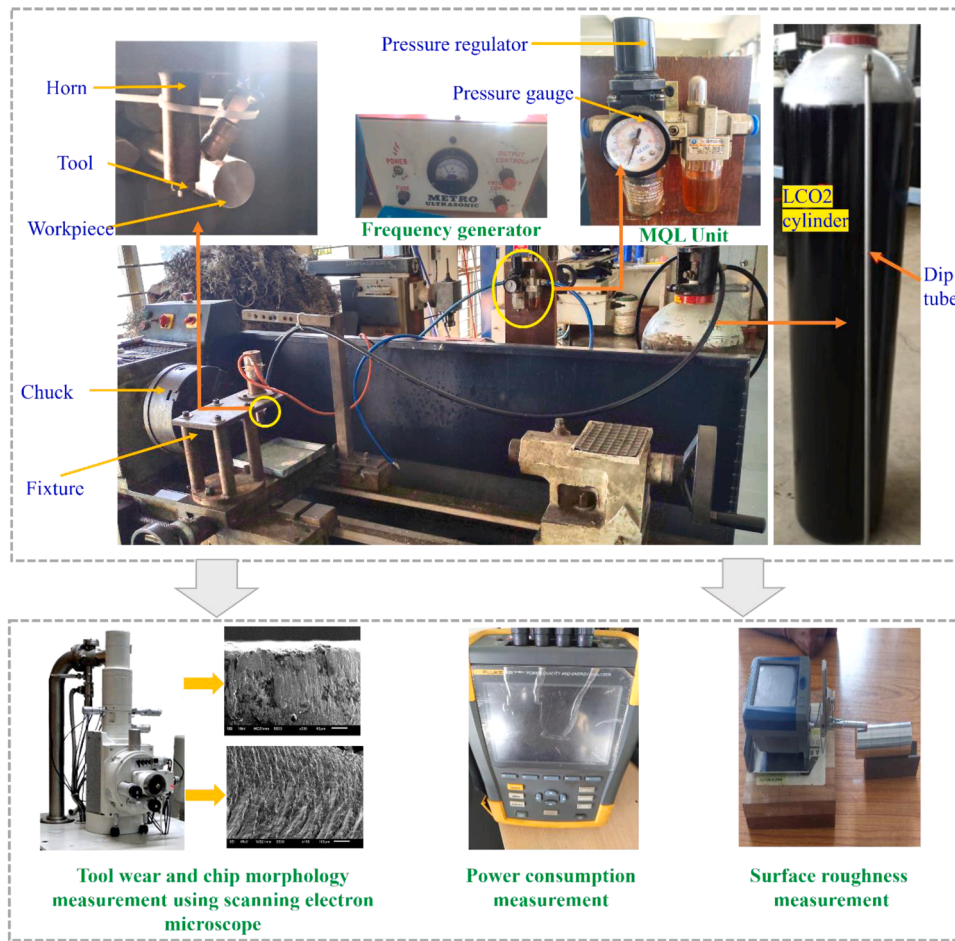
Fig. 1. An experimental setup used in this study.

transducer renovates a high-frequency electrical signal to mechanical displacement. The mechanical displacement in terms of vibration is transferred to the tool through a horn. The horn is a cylindrical stepped bar, amplifying the amplitude of vibration. The material used to make the horn is mild steel. The length of the horn is decided based on Eq. (1) [3], as follows:

$$\omega_n = \frac{\pi C}{l} \tag{1}$$

where, ω_n is the natural frequency of vibration, C is speed of sound through solid and l is length of the horn. In this study, the length of horn is 123 mm. The bigger and small diameters are 35 mm and 20 mm respectively. The tool attached, at the end of the horn, vibrates and cuts the materials simultaneously. In the present study, the resonance frequency of 20 kHz and amplitude of 10 µm is used. The frequency is applied in the tangential direction, since it gives better results. The steps followed in this study are presented in Fig. 1.

2.1. Materials

A cylindrical bar of Ti-6Al-4V having a diameter of 40 mm is used to perform the experiments. The chemical structure of this alloy is given in Table 1. The insert used is CNMG120408MS (Made: Kyocera), PVD

coated, having a nose radius of 0.8 mm, is used. It contains of a coating of TiAlN. The particulars of input process parameters and cutting conditions are given in Table 2.

Table 2
Conditions used to perform the experiment.

Parameters	Attributes
Workpiece	A cylindrical bar of Ti-6Al-4V of 40 mm diameter
Tool	CNMG 120408 with a nose radius of 0.8 mm
Rake angle	0°
Coating	PVD multilayer coating of TiAlN
Machine tool	Conventional lathe
Cutting condition	Conventional and Ultrasonic assisted turning
Frequency	20,000 Hz
Amplitude	10 µm (Peak-to-peak)
Details of the horn	Material: Mild steel, Length: 123 mm, Bigger diameter: 35 mm, Smaller diameter: 20 mm
Cutting speed	66 m/min
Feed	0.22 mm/rev
Depth of cut	0.3 mm
Length of cut	500 mm
Cutting strategies	Dry, Wet, MQL and LCO_2
Cutting fluid	Emulsion of synthetic oil
Surface roughness	Contact type surface roughness tester Taylor Hobson Surtronic S128
Power consumption	Power analyzer Fluke 435 series II
Tool wear	Scanning electron microscope JEOL 6610LV
Chip morphology	

Table 1
Chemical structure of Ti-6Al-4V.

Element	Ti	V (%)	O (%)	Fe (%)	C (%)	N (%)
wt%	Balance	4.33	5.92	0.13	0.032	0.012

2.2. Experiments

The experiments are performed using UAT and CT at different process parameters. Cutting speeds, feed, depth of cut, frequency and vibration amplitude are considered as input parameters. The values of the cutting speed can be chosen based on a value of critical cutting speed (V_c), which is given by Eq. (2) [3].

$$V < V_{cr} = 2\pi aF \tag{2}$$

Where V is cutting speed, a is amplitude, and F is frequency. The cyclic cutting is only achieved when a V is less than a V_{cr}. If Eq. (1) is not fulfilled, the cutting action becomes continuous [27]. Considering Eq. (1), the cutting speed used for experiment is 66 m/min as the critical cutting speed is 75 m/min for the resonance frequency and amplitude of 20 kHz and 10 μm, respectively. Feed and depth of cut considered are 0.22 mm/rev and 0.3 mm, respectively. The length of cut used is 50 mm. all the experiments are repeated twice to minimize the parameter error.

The turning operation is performed under dry, wet, MQL and LCO$_2$ for both the processes, i.e., conventional and ultrasonic. An emulsion-based cutting fluid is used for wet condition. As discussed earlier, this conventional cutting fluid is not suitable for sustainability, as it produces harmful gases that affect human health [28]. In contrast, the MQL and LCO$_2$ are sustainable, as it minimizes emulsion-based cutting fluid. The setup used for MQL is shown in Fig. 1. It consists of a pressure regulator, pressure gauge, oil collector and nozzle. The air compressor raises air pressure and passes through the MQL unit. The oil particles from the oil collector mixed with air, producing the mist to be supplied to the cutting area. In this study, the Canola oil is used with a 7–8 ml/h flow rate with a pressure of 5 bar. It is also seen that LCO$_2$ is suitable as a sustainable cutting fluid, as it does not affect human health and fulfills the economic and environmental criteria of sustainability [29]. The details of cooling strategies are summarized in Table 3.

2.3. Measurement of output responses

The machinability of Ti-6Al-4V is studied considering tool wear, surface roughness, power consumption and chip morphology. Total cutting length of 500 mm is considered for the flank wear. A fresh cutting edge is used for each experiment,. The measurement of tool wear is executed at the end of machining. It includes the measurement of the average maximum width of flank wear (VB), and morphology of tool flank and crater wear. A scanning electron microscope (Make: Jeol, Model:6610 LV)is used to analyze the morphology flank and crater wear. According to the criteria given by ISO 3685:1993, the maximum width of the flank wear should not be greater than 0.3 mm [27]. Furthermore, the power consumption is measured by Fluke 435 power analyzer, as shown in Fig. 1. The device is connected with 3 phase power connector. A contact-type surface roughness tester (Make: Taylor Hobson, Model: Surtronic S128) is employed to determine the average surface roughness, as exposed in Fig. 1. The cut-off and evaluation length used are 0.8 mm and 4 mm, respectively. For each experiment, total 3 profiles are considered for the analysis. After each experiment, the chips

Table 3
Details of cooling strategies employed.

Parameter	Attributes
Wet cooling	Fluid: Emulsion of synthetic oil in water, Pressure: 3 bar, Flow rate: 21 l/min, Nozzle diameter: 10 mm,
MQL	Oil: Canola oil, Pressure of air: 5 bar, Flow rate: 7–8 ml/h, Nozzle diameter: 2 mm,
LCO$_2$	Pressure of the cylinder: 57 bar, flow rate: 27 l/h, Nozzle diameter: 2 mm
Distance of nozzle tip from rake face	20 mm for all the cooling strategies

are collected. The chip morphology is investigated using an electron microscope.

3. Results and discussions

The tool wear is the most significant factor in analyzing the machinability of materials. Moreover, it directly affects the cutting force, power consumption, surface finish, chip morphology, etc., during machining. In this regard, the morphology of tool wear is analyzed, and the results are discussed in the subsequent subsections. The tool wear, surface roughness, power consumption, specific cutting energy, and chip morphology are deliberated in the subsequent subsections.

3.1. Flank wear

An average width of the flank wear (VB) is measured at three different locations of the tool using a scanning electron microscope, as displayed in Fig. 2(a). VB An average value of VB in CT and UAT under different cooling environments is revealed in Fig. 2(b). Compared to the CT, the UAT shows an approximate reduction of 27%, 26% and 31% in VB under wet, MQL and LCO$_2$. The CT shows an approximate reduction of 29% and 53% in VB under MQL and LCO$_2$, compared to dry condition. The UAT shows an approximate reduction of 35%, 54% and 70% in VB under wet, MQL and LCO$_2$, compared to dry condition. The CT shows a lower value VB than UAT, under dry condition. On the other hand, the UAT is better than CT, under wet, MQL and LCO$_2$. It can also be detected that, the VB is slightly higher in CT under wet condition than dry condition, whereas it is significantly lower in UAT under wet condition than dry condition. Under MQL and LCO$_2$, the VB shows a significant reduction compared to dry and wet conditions, in both the processes. Due to higher cutting temperature in the dry condition, the VB is higher in the UAT under dry condition [22]. Moreover, due to vibration in UAT, extra heat is also added, enhancing the wear rate in dry condition. Alternatively, in CT, the VB is slightly lesser in dry condition than in wet condition. It may be attributed to a chemical affinity of Ti-6Al-4V with coolant used for wet condition, progressing the wear rate and showing the higher value of VB [20]. In UAT, during the disengagement period, heat dissipates from cutting zone and lessens the temperature, lowering the tendency of chemical reaction of Ti-6Al-4V with the coolant. A reduction in the VB is due to the effect of cooling and lubrication under both the conditions. Oil particles in MQL form a lubricative layer at the tool-workpiece interface, lowing the interaction and reducing the VB. The LCO$_2$ drops the cutting temperature significantly and retains the hardness of the tool for a longer time [17]. Therefore, the VB is lesser under LCO$_2$ under both the processes.

The morphology of flank wear observed in CT and UAT under different cooling strategies is exposed in Fig. 3. The CT under dry condition shows a built-up edge (BUE), abrasion, adhesion, and peeling off the coating on the flank face, as revealed in Fig. 3(a). On the other hand, in UAT under dry condition, the BUE and adhesion are not severe. However, abrasion and chipping of cutting edge are observed, as shown in Fig. 3(b). Low heat conductivity and chemical reactivity of Ti-6Al-4V with the tool material, generating a high temperature and causing a BUE formation and adhesion [30]. When the adhered material is removed, it brings a tool material with it, resulting in an edge chipping, as shown in UAT. According to Biksa et al. [31], the BUE is associated with attrition, resulting in chipping of the cutting edge, mainly in intermittent cutting. The tool repetitively separates with the workpiece generating an interrupted mode of cutting, increasing the tendency of edge chipping. A high heat generation in the deformation zone, in dry condition, peeling off the coating of TiAlN at high temperature, exposing the substrate to a workpiece. Exposure of substrate to workpiece causes abrasion, increasing the flank wear [32]. The abrasion observed in the UAT seems less severe than in CT. The vibrations add additional heat but lessen the tool-workpiece contact area, decreasing the abrasion. Ultimately, it can be noted that abrasion and adhesion are the main tool wear mechanism
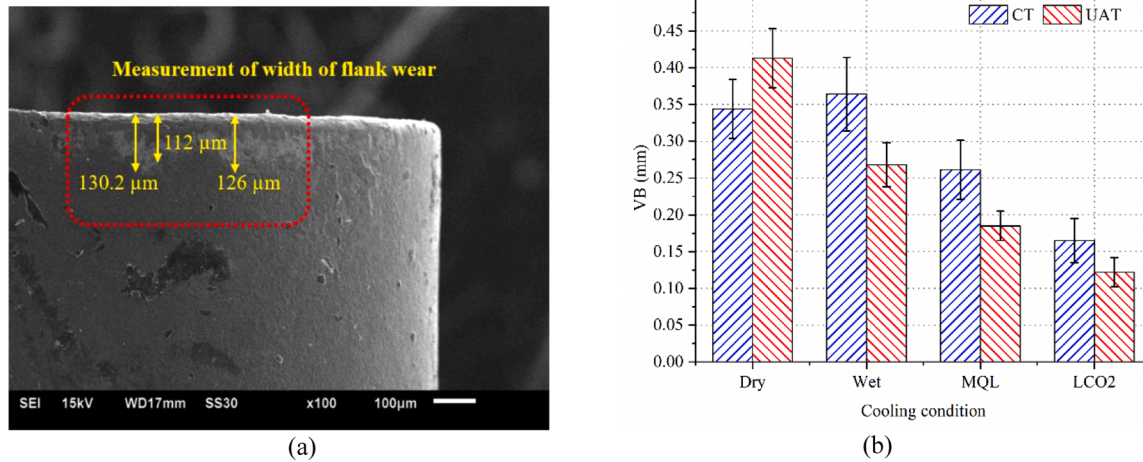
Fig. 2. (a) Measurement of width of flank wear (*UAT under LCO$_2$*) and (b) Average width of flank wear measured under different cooling strategies.

observed in machining of Ti-6Al-4V under dry condition.

The CT shows substantial flank wear under wet condition, as observed in Fig. 3(c). The flank wear is higher under wet conditions than dry conditions. On the other hand, the UAT shows a drastic lessening in flank wear compared to dry and the CT under wet conditions. A BUE, adhesion of workpiece material and abrasion, are severe in the CT, whereas they look mild in the UAT, as shown in Fig. 3(d). Some microparticles adhere on the flank face and peeling of coating is taken place near the cutting edge. The wet condition could not prevent the adhesion of workpiece material due to the reactivity of titanium with the tool. It is found that during the machining of titanium alloy, the additives in the cutting fluid react with the titanium. This chemical reaction causes abrasion on the flank face [33]. Additionally, the aluminum of TiAlN coating also reacts with the oxygen from the atmosphere and creates aluminum oxide, reacting rapidly with the titanium. As aluminum oxide has the least resistance of abrasion causing abrasive wear [34]. In the UAT, the chemical reaction is not as severe as in CT, eliminating the abrasion. Moreover, cutting fluid lowers the temperature in the deformation.

zone and decreases the adhesion due to ultrasonic vibration in the UAT. Thus, using ultrasonic vibration, the flank wear can significantly be reduced than CT even under flood cooling condition.

The CT under MQL shows almost a similar nature of flank wear as that in wet condition. On the other hand, the UAT shows a reduction in flank wear compared to dry and wet conditions. In the CT, the BUE formation, adhesion and abrasion are observed, as exposed in Fig. 3(e). The size of BUE seems reduced under MQL than under wet condition. Furthermore, the adhesion and abrasion appear near the cutting edge and at the tool nose, respectively. As displayed in Fig. 3(f), a small adhesion and peeling off the coatings are noted in the UAT compared to the CT. The MQL reduces the abrasion due to oil particles between the tool and workpiece, lowering the friction and heat [35]. However, the MQL is insufficient to minimize the adhesion, particularly in the CT due to the continuous contact. Owing to the poor heat conductivity of Ti-6Al-4V, the temperature at the cutting zone is very high, activating the ions of the oil particles. These ions then react with freshly generated workpiece surface, increasing the possibility of adhesion [36]. The lack of cutting fluid near the cutting edge and tool nose provides the conductive condition for workpiece and micro fragments to cause the abrasion [17]. Ultrasonic vibrations combined with MQL significantly suppress adhesion and abrasion. This is attributed to an improvement in cooling and lubrication of MQL because of intermittent cutting. During the disengagement period in UAT, the oil particles can penetrate into the cutting zone, removing the heat and lowering the tool wear.

The LCO$_2$ shows a substantial reduction in flank wear as compared to

other strategies, in both the processes. It also eliminates BUE formation in the CT, unlike in dry, wet and MQL. A small adhesion on the flank face and a minor abrasion and edge chipping are noted in the CT, as shown in Fig. 3(g). On the other hand, a minor abrasion and edge chipping at the cutting edge are realized in the UAT, as given in Fig. 3(h). The chipping is attributed to the thermo-mechanical load fluctuation at the cutting edge. Poor heat conductivity of Ti-6Al-4V generates a large heat; simultaneously, the LCO$_2$ reduces the temperature, producing a thermal load at the cutting edge and causing an edge chipping [37]. Furthermore, the segmented chips formed during machining of Ti-6Al-4V induce very high stresses at the cutting edge, causing an edge chipping. The TiAlN is insufficient to sustain a thermal and mechanical load and wears out rapidly by abrasion, mainly in CT. In the UAT, the ultrasonic vibration further enhances the mechanical stresses imposed on the cutting edge and increases the chipping. Thus, the edge chipping seems a bit larger in the UAT than the CT. Similar observations have been made for the machining of Ti-6Al-4V under cryogenic cooling by Agrawal et al. [21]. Eventually, it can be said that LCO$_2$ is much more effective in machining Ti-6Al-4V in CT and UAT processes.

3.2. Crater wear

The chips sliding over the rake face significantly damages the rake face by causing high friction, stress and temperature. Thus, the rake face wear takes place. The morphology of crater wear observed in CT and UAT under different cooling strategies are presented in Fig. 4.

As exposed in Fig. 4(a), the CT under dry condition produces BUE, severe abrasion and crater. Unlike in the CT, the UAT suppresses the BUE, as shown in Fig. 4(b). However, the abrasion, adhesion and peeling off the coatings are observed in both the condition in almost all the strategies. The chemical reactivity and poor heat conductivity of Ti-6Al-4V lead to BUE formation and adhesion on the rake face. Moreover, segmented chip formation during machining imposes higher stresses at the cutting edge, and welding of the chip with the rake face takes place. In the subsequent machining, when the chip adheres to the cutting edge is removed, it brings particles of tool materials and the formation of a crater occurs [30]. Moreover, the coating of TiAlN no longer sustains such high stresses and temperature (up to 900 °C [38]), allowing to diffuse the carbon into the chip, forming a crater. Thus, a crater is also formed due to the diffusion mechanism, mainly during the machining of titanium in dry condition [15,21]. As long as the temperature is very high at the cutting edge, the coating becomes soft and wears out more rapidly with abrasion. Ultrasonic vibration reduces the adhesion and formation of BUE by improving the chip breakability. However, the tool particles sandwiched between chip and tool form wear by abrasion
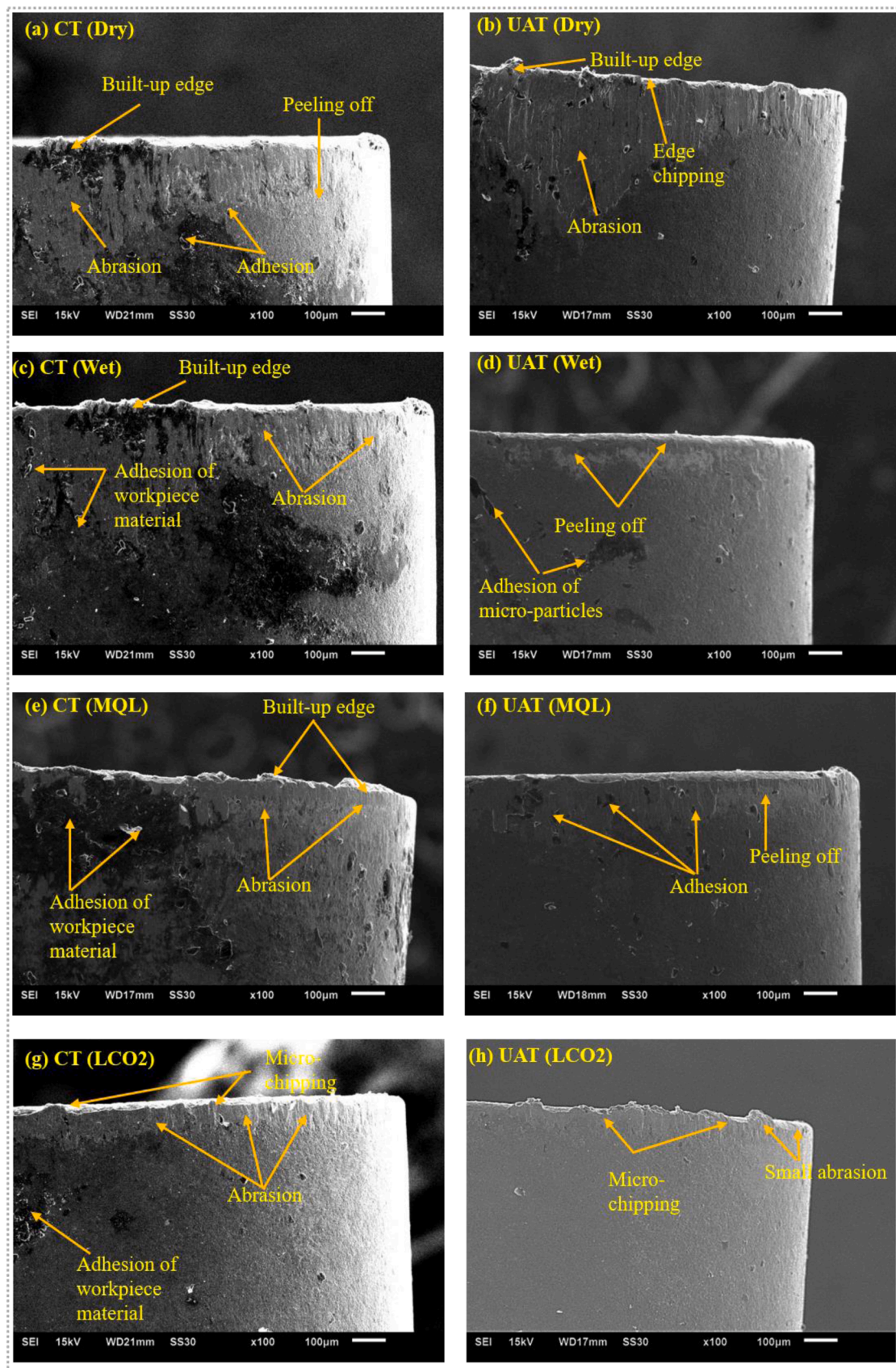
Fig. 3. Morphology of flank wear observed in CT under (a) dry, (c) wet, (e) MQL and (g) LCO$_2$, and UAT under (b) dry, (d) wet, (f) MQL and (h) LCO$_2$.
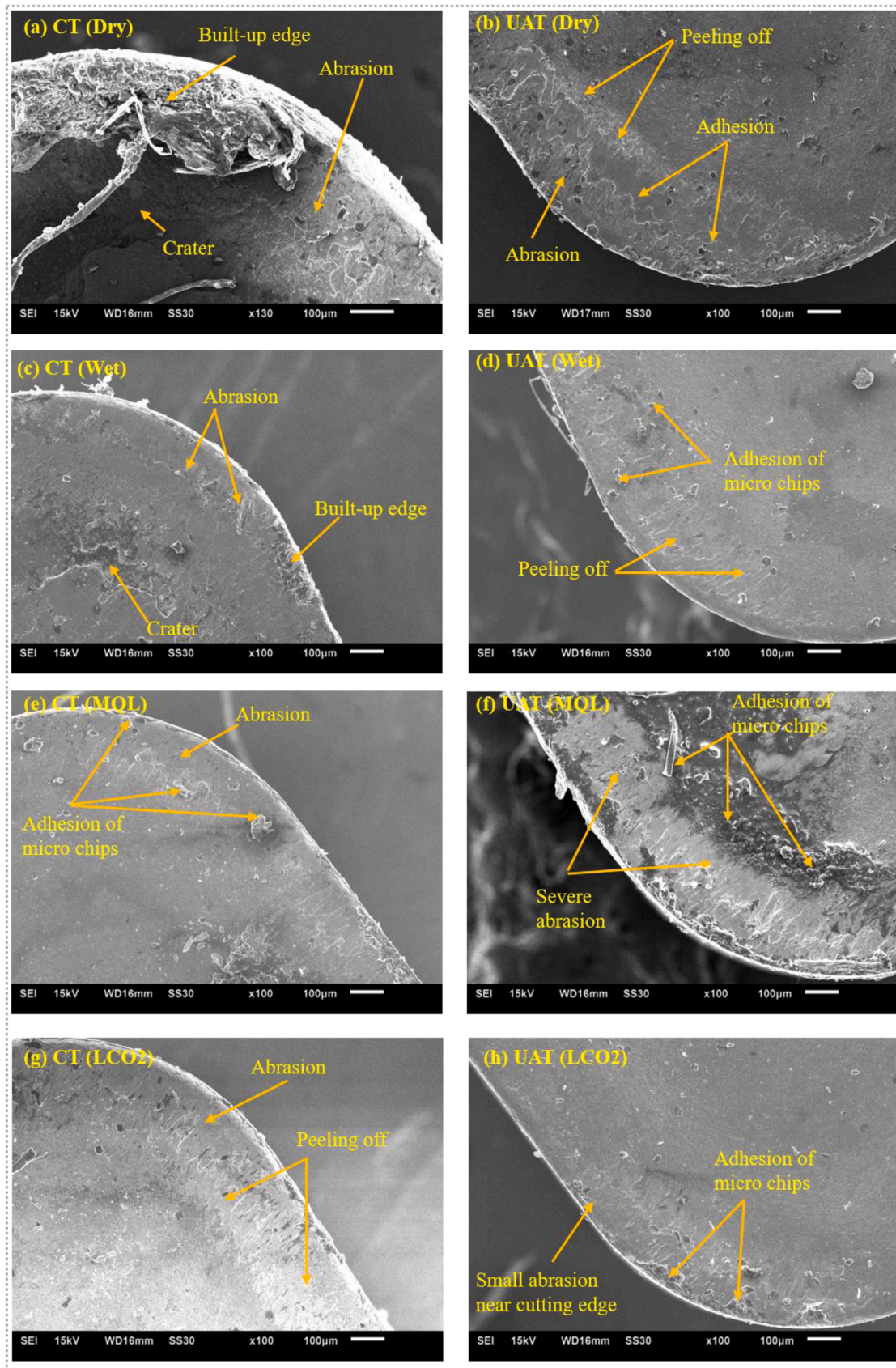
Fig. 4. Morphology of crater wear observed in CT under (a) dry, (c) wet, (e) MQL and (g) LCO$_2$, and UAT under (b) dry, (d) wet, (f) MQL and (h) LCO$_2$.

under high pressure and temperature, even in UAT. The peeling of the coating is mainly noted at a sleeping zone of the tool-chip contact area.

The wet condition minimizes the BUE formation, abrasion, and adhesion compared to that in dry condition, in both the processes. As shown in Fig. 4(c), an abrasion, a small BUE and a crater are observed in the CT, whereas adhesion of small microchips and peeling off the coating are observed in the UAT, as shown in Fig. 4(d). Thus, the UAT lowers the abrasion and adhesion compared to the CT. The wet condition provides sufficient cooling and eliminates the heat from the machining zone, reducing stresses and temperature and eventually lowering the wear than in dry condition [39]. Yet, the coolant is not effectively reached at the cutting edge, forming a small BUE. Due to uneven cooling near the cutting edge, thermal stresses are imposed, reducing.

the strength of the coating and cobalt binder. Therefore, the tool materials remove by the chips flow over the rake face, forming a crater by abrasion. Additionally, the chip chemically reacts with the carbon in the tool, forming an interlayer of titanium carbide. This interlayer strongly bonds with chip and tool, endorsing seizure by the diffusion and producing a crater [34]. The UAT allows the cutting fluid to reach near the edge, dissipating the heat during the disengagement period. Furthermore, in the UAT, pulsating forces and stresses imposed on the tool, reducing the average stresses and pressure on the rake face. Thus, the strength of the tool retains for a longer time, reducing the crater wear.

As shown in Fig. 4(e), the MQL shows better results of tool wear on the rake face than in dry and wet conditions for the CT. On the contrary, the tool wear significantly increases in the UAT under MQL, as shown in Fig. 4(f). The abrasion, adhesion and formation of BUE are decreased in the CT, whereas they are significantly higher in the UAT. The oil particles in MQL form a lubricating layer at interface area, lowering the friction and heat in the machining zone [40]. According to Chetan et al. [41], the contact angle made by biodegradable oil on the surface of Titanium is relatively lower than other surfaces, improving the wetting capability and enhancing the lubrication. Therefore, an abrasion and adhesion decrease under the MQL. In the case of UAT, implying ultrasonic vibration itself generates heat and mechanical load at the cutting edge. Moreover, less quantity of fluid used in MQL is insufficient to disperse the heat from the tool-chip interface. Additionally, the compressed air used in MQL, might produce more friction at tool-chip contact zone, showing more abrasion compared to dry condition. Eventually, the cutting edge becomes soft due to a large heat generation and wear of coating occurs due to abrasion. Similar observations are made for ultrasonic-assisted side milling of Ti-6Al-4V under MQL by Ni et al. [11]. Thus, it can be said that the UAT is inferior under MQL in reducing tool crater wear than CT.

The LCO_2 shows a superior performance in terms of abrasion, adhesion and BUE compared to other strategies, in both the processes. Fig. 4(g) shows that small abrasion and peeling off the coatings is mainly observed at the tool-chip contact area. Alternatively, the UAT greatly losses the abrasion and adhesion compared to the CT, as shown in Fig. 4 (h). The abrasion and adhesion of small microchips are primarily noted at the cutting edge and tool nose part. The LCO_2 lowers the cutting temperature retaining the hardness of the tool lowering the abrasion [19]. However, the shear localized chip formation in titanium machining induces a larger load at a cutting edge and tool nose. Eventually, the abrasion and peeling of the coating happen. In the UAT, the cyclic cutting nature of the tool reduces the load imposed by the shear localized chip on the cutting edge, decreasing tool-chip contact length and seizure zone. Moreover, it also allows the LCO_2 to penetrate at tool-chip interface, removing the heat and lessening the thermal load to the cutting edge. Ultimately, it reduces abrasion and adhesion on the rake face. In this regard, Sadik and Isakon [37] have noted in the milling Ti-6Al-4V that LCO_2 eliminates chipping and abrasion due to effective cooling. Ultimately, it can be said that LCO_2 is superior in decreasing the tool wear compared to other strategies, for both the processes. Additionally, the UAT further decreases the tool wear under LCO_2 attributed

to intermittent cutting characteristics.

3.3. Power consumption

The power consumption during machining provides the stability of the process and helps to categorize optimum parameters for reducing energy consumption. To achieve sustainability in the machining process, the power consumption during machining should be minimized. This section analyzes the power consumed by machine tools during CT and UAT under different cutting environments. Fig. 5 represents the power consumed in CT and UAT under different cooling strategies. The dry and LCO_2 conditions show a lower power consumption value than wet and MQL conditions. The UAT does not show a significant variation in power consumption in all the conditions. In the dry conditions, it is observed that the BUE formation is higher than in other conditions, acting as another cutting edge, lowering the tool-chip contact length and forces and ultimately power consumption [17,42]. A reduction in machining force in UAT is owing to the pulsating cutting forces, reducing the average machining forces and power consumption [43]. The wet condition uses an external pump to flow the cutting fluid at the rake face during machining. Thus, adding the power required for machining and the external pump gives the total power for the wet condition. In the case of MQL, the power required to run the compressor is used to blow the air along with oil particles at the cutting zone. Thus, the total power required for machining under MQL becomes higher than in other conditions. When it comes to LCO_2, no external component is used other than a cylinder of LCO_2. In this regard, the power consumption could be lesser in machining under LCO_2. On the other hand, an effective cooling provided by LCO_2 deliberately reduces the tool-chip contact length, friction at the cutting zone and heat, decreasing the power consumption in CT and UAT under LCO_2. Quantitatively, an average drop in power consumption for the CT under LCO_2 is 15%, 30% and 60% compared to dry, wet and MQL conditions. Similarly, an average reduction in power consumption for the UAT under LCO_2 is 10%, 32% and 58% compared to dry, wet and MQL conditions.

3.4. Surface roughness

The machined surface quality is mainly influenced by workpiece material, tool material and geometry, cutting zone temperature, chip geometry, cutting fluid, etc [44,45]. Higher surface quality reduces the rejection of the part. Typically, average surface roughness (R_a) is used to check the feature of the machined surface. In the present study, the R_a is
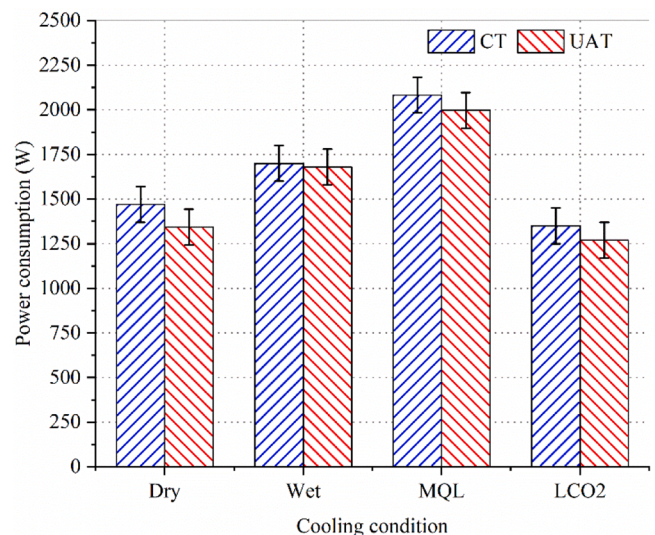

Fig. 5. Power consumption measured in CT and UAT under different cooling strategies.

measured on the machined surface at the end of machining in all the conditions and, the results are revealed in Fig. 6. It can be observed that the R_a is maximum in dry conditions compared to wet, MQL and LCO$_2$ for both the processes. The UAT shows a significant reduction in R_a mainly under wet and LCO$_2$. The R_a does not much differ both the processes, under dry and MQL conditions. Moreover, under dry and wet conditions, the difference between the R_a in CT is not significant, whereas, it is significant in case of the UAT. The tool wear is higher in dry conditions, deteriorating the surface quality. Moreover, the adhesion and abrasion take place on the tool, increasing the friction at tool-workpiece interface, raising the heat and lowering the surface quality [43]. Compared to dry condition, the wet condition slightly reduces the R_a in the CT, whereas it reduces deliberately in the UAT. This is ascribed to the tool wear, which is more in the case of CT than in UAT. The higher tool wear in the CT reduces the surface quality and increases the R_a. The abrasion and adhesion of microparticles are responsible for degrading the surface quality in the CT. On the other hand, very less amount of tool wear in the UAT reduces the R_a. During the ultrasonic vibration, the cutting fluid can penetrate between the tool-workpiece and tool-chip contact area, removing the heat from the machining zone, improving the surface quality [3]. The MQL shows better results of R_a Compared to dry and wet conditions. However, the difference between R_a in CT and UAT is not noteworthy. A reduction in R_a is owing to evaporative cooling and lubricating properties. The former makes the tool-chip and tool-workpiece interface cooler, and the latter lowers the coefficient friction at secondary and tertiary shear zone. In addition to that, the pressurized airflow enforcing the chips to remove from the newly generated machined surface, improving the surface quality [46]. An ultrasonic vibration further enhances the surface quality by improving cooling and lubrication at the cutting zone during machining. The LCO$_2$ is superior in improving the surface quality compared to other strategies for both the processes. A drastic lessening in tool wear resulted in an improved surface quality under LCO$_2$. Besides, the tool-chip contact length is much lesser during machining under LCO$_2$ than under dry, wet, and MQL lessening the friction at the secondary zone and reducing the heat and forces. Eventually, the surface quality improves under LCO$_2$ [47]. Moreover, LCO$_2$ provides sufficient cooling, which prevents thermal softening of the tool, chipping of the cutting edge, and ultimately reduces the R_a. The UAT under LCO$_2$ is much more effective in improving the surface quality. Due to the intermittent cutting characteristic between tool and workpiece in the UAT, it reduces the stresses imposed on the tool and chip breakability, which reduces the frictional

heat and improves the surface quality [3]. Quantitatively, an average reduction in R_a for the CT under LCO$_2$ is 30%, 25% and 12% compared to dry, wet and MQL conditions. Similarly, an average reduction in R_a for the UAT under LCO$_2$ is 43%, 24% and 22% compared to dry, wet and MQL conditions.

3.5. Variation in specific cutting energy and surface roughness with tool wear

The economy of the machining processes is primarily reliant upon the energy consumption in machining. The energy consumption during machining affects the sustainability goals. Thus, it is required to reduce the energy consumption achieving good machinability of the materials. The Specific Cutting Energy (SCE) criterion evaluates the energy consumption during machining. The SCE is a ratio of power consumption during machining to the material removal rate, as given by Eq. (3),

$$SCE = \frac{P_M}{MRR} \tag{3}$$

where, P_M is power consumed during machining in watt. It is determined by subtracting the ideal power of machine from total power, as follows,

$$P_M = P_T - P_I \tag{4}$$

where, P_T and P_I are total power and ideal power, respectively. The MRR is determined using Eq. (5),

$$MRR = V \times a_p \times f \tag{5}$$

where, V is cutting speed, f is feed and a_p is depth of cut. A variation in SCE and average surface roughness (R_a) with tool wear for CT and UAT is noted in Fig. 7. It is noted that the SCE is the lowest and R_a is higher in CT and UAT under dry condition. The dry condition does not use fluid; thus, no external equipment is needed to lower the SCE. At the same time, the higher value of R_a is noted due to higher tool wear. The UAT requires a slightly less SCE though the tool wear and R_a is slightly higher than CT under dry condition. The wet condition has a higher SCE than dry condition due to more power consumption. The CT increases the SCE as the tool wear increases. Conversely, the UAT also raises the SCE though the tool wear decreases. The R_a is slightly reduced in CT though the tool wear increases, whereas the UAT shows a considerable reduction in R_a with tool wear [48,49]. The SCE in the MQL is highest among all the cooling strategies for both processes. An increment in SCE is due to the power consumption, which is highest for MQL in both the processes. On the other hand, MQL shows a substantial lessening in tool wear and R_a, yet the SCE is the highest. A reduction in R_a and tool wear in machining under MQL is already discussed in the previous subsections. The LCO$_2$ reduces the need drastically in both the processes. Additionally, it also decreases the tool wear and R_a, with a reducing in SCE. The LCO$_2$ system does not require any external equipment other than a cylinder of LCO$_2$. Moreover, the effectiveness of LCO$_2$ in reducing the R_a and tool wear has been already discussed previously. The UAT along with LCO$_2$ further reduces a requirement of SCE without the cost of tool wear and R_a. Thus, to attain sustainability, the LCO$_2$ and ultrasonic vibration are better among all other cooling strategies. A similar conclusion is also made during the machining of Ti-6Al-4V under LN$_2$ by Agrawal et al. [21].

3.6. Chip morphology

Segmented chips formation is a typical characteristic of titanium alloy. Segmented chips are mainly responsible for a periodic variation in cutting force and stresses, reducing the tool life and surface quality. This segmentation or shear localization in the chips could be due to an instability of plastic deformation, variation in physical and metallurgical changes, etc. [50]. In this study, the chips formed during CT and UAT of Ti-6Al-4V under dry, wet MQL and LCO$_2$ are collected and analyzed. As
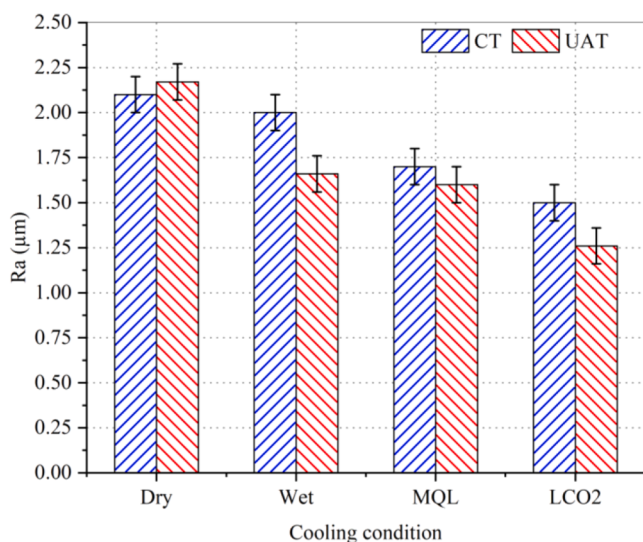

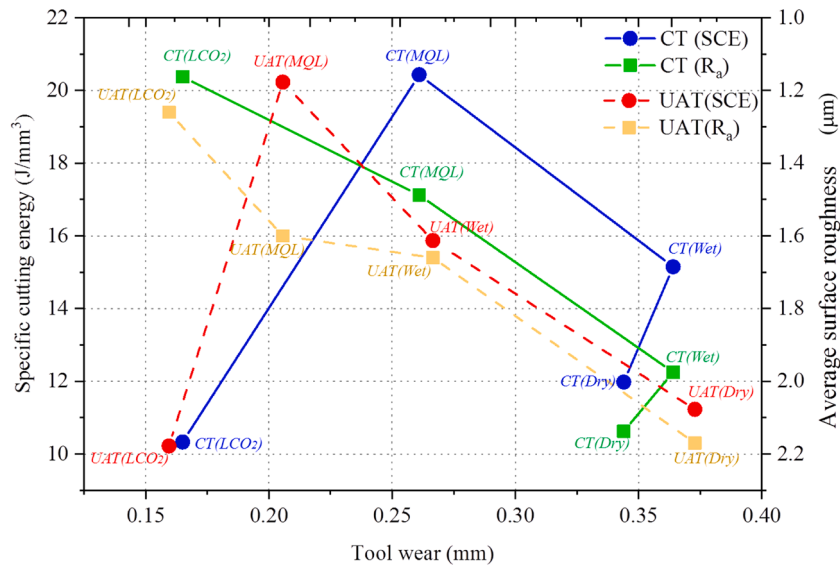**Fig. 6.** Average surface roughness measured in CT and UAT under different cooling strategies.

Fig. 7. Variation in specific cutting energy and average surface roughness with tool wear during CT and UAT under different cooling strategies.

shown in Fig. 8, the chip geometry is examined macroscopically, whereas; morphology is examined under SEM. As shown in Fig. 8(a), the chips seem very long, irregular, and nonuniform in the CT under dry condition. In the dry condition, the heat generation at primary and secondary deformation zone is higher due to lack of cooling, increasing tool-chip contact length and friction producing nonuniform chips.

Unlike the CT, the UAT produces discontinuous chips, as shown in Fig. 8 (b). An ultrasonic vibration lowers the tool-chip contact length due to the periodic disengagement of the tool and workpiece, reducing the friction and producing discontinuous chips [51]. Moreover, it is also noted that chips formed in the UAT have fine lamella structure compared to CT. The vibration helps to propagate the crack produced,
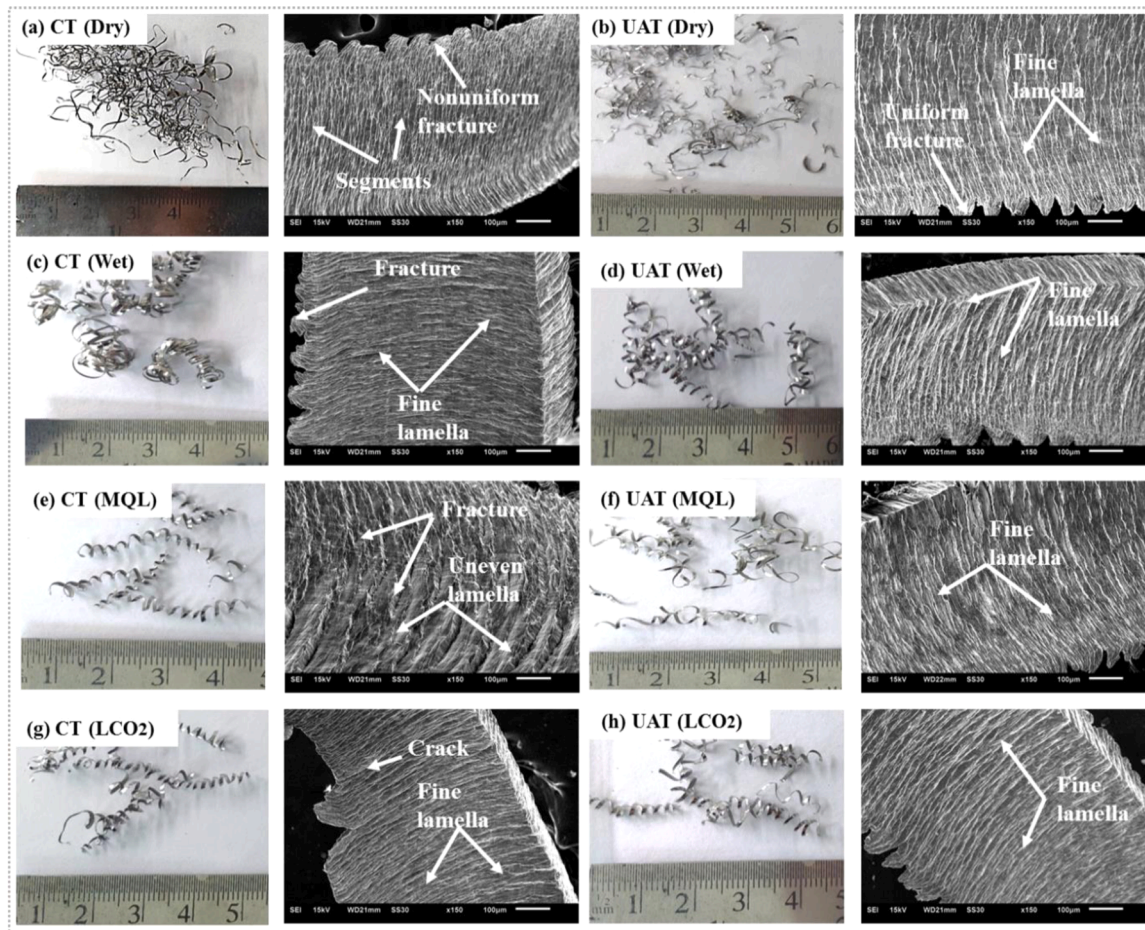

Fig. 8. Chips geometry and morphology observed in CT under (a) dry, (c) wet, (e) MQL and (g) LCO$_2$, and UAT under (b) dry, (d) wet, (f) MQL and (h) LCO$_2$.

producing the chips with uniform fracture. The wet condition shows continuous spiral chips in the CT, whereas the chips are comparatively shorter with a large curling radius in the UAT. As shown in Fig. 8(c), the chips show nonuniform fracture with a fine lamella structure in the CT. The cutting fluid facilitates the shear band formation enhancing the chip morphology and producing the chips with fine lamella [37]. It can be depends upon the heat generation and friction at deformation zone. A reduction in temperature and friction produces the chips with a fine lamella. In the UAT, the cutting fluid penetrates between tool and chip, further lowering the friction and improving the chip morphology. In the case of MQL, the chips produced are of lower curling radius and short length in the CT, as shown in Fig. 8(e). The MQL makes chip removal easier by providing a high-pressure airflow between tool and chip. Moreover, the oil particles decrease the friction by forming a lubricating layer between tool and chip, making chip removal easy. However, due to insufficient cooling at the tool-chip contact length in the CT, the chips show an uneven lamella structure with a fractured surface. In the MQL due to insufficient cooling the friction is higher, increasing the temperature, producing fractured chips with uneven lamella. The UAT formed the chips with a shorter length and curling radius than CT, as shown in Fig. 8(f). Ultrasonic vibration and pressurized air improve the chip breaking effect, producing chips with a fine lamella. A similar observation has been made in ultrasonic-assisted milling of Ti-6Al-4V by Ni et al. [11]. The CT and UAT, under LCO_2 produce the chips with shorter length. As presented in Fig. 8(g), the CT shows a chip with a fine lamella structure. The crack shown may be due to the thermal load generated due to the heat and cooling effect of LCO_2. It can be explained by a reduction in tool-chip contact length due to the pressurized flow of LCO_2, extracting the heat from the secondary shear zone. Therefore, less heat is dissipated to the tool, reducing the tool wear and forming the chips with a fine lamella structure [52]. This mechanism is more effective in the UAT due to the intermittent cutting characteristic between tool and workpiece, producing very fine structured chips, as shown in Fig. 8(h). Thus, it can be said the machining performance can be upgraded using the simultaneous effect of ultrasonic vibration and LCO_2.

4. Summary

Table 4 describes the comparison of LCO_2 with dry, wet and MQL for CT and UAT of Ti-6Al-4V. It may be noted that the LCO_2 performs better than other strategies in reducing flank and crater wear, surface roughness, power consumption and specific cutting energy, and improving the chip morphology. Moreover, the UAT under LCO_2 performs better than CT for all the outcomes. Thus, it can be said that the LCO_2 with UAT is more favorable to achieve sustainability in the machining of Ti-6Al-4V.

5. Conclusions

This work demonstrates the machining of Ti-6Al-4V using conventional and ultrasonic-assisted turning performed under dry, wet MQL and LCO_2. The novelty of this work is a combination of MQL and LCO_2 with the UAT process. The morphology and behavior of tool wear are analyzed and compared for CT and UAT under different cooling strategies. The effect of tool wear on the machinability of Ti-6Al-4V in terms of power consumption, average surface roughness and chip morphology is also studied. Based on the results discussed above, the following is concluded:

- The main flank wear mechanisms observed are abrasion, adhesion and BUE in the CT and UAT. The LCO_2, along with ultrasonic vibrations, eliminates the BUE formation and flank wear. The UAT shows an approximate reduction of 35%, 54% and 70% in average width of flank wear under wet, MQL and LCO_2, compared to dry condition.
- Diffusion, abrasion, adhesion, and chipping are the main mechanisms observed for tool crater wear in dry conditions. The wet, MQL and LCO_2 deliberately reduce the crater wear by enabling heat dissipation. The effective cooling provided by LCO_2 significantly minimizes the crater wear for CT and UAT.
- An average reduction in average surface roughness for the CT under LCO_2 is 30%, 25% and 12% compared to dry, wet and MQL conditions. Similarly, for the UAT under LCO_2, it is 43%, 24% and 22% compared to dry, wet and MQL conditions.
- An average reduction in power consumption for the CT under LCO_2 is 15%, 30% and 60% compared to dry, wet and MQL conditions. Similarly, for the UAT under LCO_2, it is 10%, 32% and 58% compared to dry, wet and MQL conditions.
- The chips produced under LCO_2 are shorter and have fine lamella structured in both the conditions. It is owing a reduction in tool-chip contact length and friction during machining under LCO_2.
- The LCO_2 with UAT significantly reduces specific cutting energy without any compromise in tool wear and surface quality. The LCO_2 may attain the sustainability goal without compromising the machinability of Ti-6Al-4V.
- The UAT under LCO_2 shows a substantial enhancement in the machinability. It is attributed to the intermittent cutting characteristic between tool and workpiece, reducing average cutting forces, tool-chip contact length and improving chip breakability. Thus, it can be concluded that the UAT under LCO_2 promotes sustainability in the machining of Ti-6Al-4V.

Table 4
Comparison of LCO_2 with other cooling strategies for CT and UAT of Ti-6Al-4V.

Machining Evaluation criteria	% Reduction with LCO_2				Novelty with UAT	Remark
	Cutting strategy	*Dry*	*Wet*	*MQL*		
Flank wear	**CT**	53	56	38	Except for wet condition, it performed better than CT	Reduced adhesion and abrasion
	UAT	68	52	28		
Crater wear	Crater wear was lesser in LCO_2 compared to dry, wet and MQL, in CT and UAT				Except for MQL, it performed better than CT	Reduced diffusion, chipping, and adhesion
Power consumption	**CT**	15	30	60	Improved surface quality than CT	Improved surface quality
	UAT	10	32	58		
Surface roughness	**CT**	30	25	12	Reduced power consumption compared to CT	Reduced power consumption
	UAT	43	24	22		
Specific cutting energy	Specific cutting energy requirement for LCO_2 was lesser compared to other strategies for CT and UAT				Reduced specific cutting energy without compromising performance compared to CT	Lowest specific cutting energy among all the strategies
Chip morphology	Chips produced during machining under LCO_2 were comparatively thin and shorter				Improved chip breakability and morphology compared to CT	Better chip morphology due to efficient cooling

Declaration of Competing Interest

The authors declare that they have no known competing financial interests or personal relationships that could have appeared to influence the work reported in this paper.

Acknowledgement

References

[1] Ezugwu EO, Wang ZM. Titanium alloys and their machinability—a review. J Mater Process Technol 1997;68:262–74.

[2] Shah P, Khanna N, Singla AK, Bansal A. Tool wear, hole quality, power consumption and chip morphology analysis for drilling Ti-6Al-4V using LN_2 and LCO_2. Tribol Int 2021;163:107190.

[3] Airao J, Khanna N, Roy A, Hegab H. Comprehensive experimental analysis and sustainability assessment of machining Nimonic 90 using ultrasonic-assisted turning facility. Int J Adv Manuf Technol 2020;109:1447–62.

[4] Jeong HI, Lee CM. A study on improvement of tool life using a heat shield in laser assisted machining to Inconel 718. Opt Laser Technol 2021;142:107208.

[5] Liang X, Liu Z, Liu W, Wang B, Yao G. Surface integrity analysis for high pressure jet assisted machined Ti-6Al-4V considering cooling pressures and injection positions. J Manuf Process 2019;40:149–59.

[6] Bai W, Bisht A, Roy A, Suwas S, Sun R, Silberschmidt VV. Improvements of machinability of aerospace-grade Inconel alloys with ultrasonically assisted hybrid machining process. Int J Adv Manuf Technol 2019;101:1143–56.

[7] Zhang P, zhang X, Cao X, Yu X, Wang Y. Analysis on the tool wear behaviour of 7050-T7451 aluminum alloy under ultrasonic elliptical vibration cutting. Wear 2021;466–467:203538.

[8] Lotfi M, Amini S, Akbari J. Surface integrity and microstructure changes in 3D elliptical ultrasonic assisted turning of Ti-6Al-4V: FEM and experimental examination. Tribol Int 2020;151:106492.

[9] Zhang L, Hashimoto T, Yan J. Machinability exploration for high-entropy alloy FeCrCoMnNi by ultrasonic vibration-assisted diamond turning. CIRP Ann Manuf Technol 2021;70:37–40.

[10] Peng Z, Zhang X, Zhang D. Effect of radial high-speed ultrasonic vibration cutting on machining performance during finish turning of hardened steel. Ultrasonics 2021;111:106340.

[11] Ni C, Zhu L, Yang Z. Comparative investigation of tool wear mechanism and corresponding machined surface characterization in feed-direction ultrasonic vibration assisted milling of Ti–Al–4V from dynamic view. Wear 2019;436–437:203006.

[12] Gao H, Ma B, Zhu Y, Yang H. Enhancement of machinability and surface quality of Ti-6Al-4V by longitudinal ultrasonic vibration-assisted milling under dry conditions. Measurement 2022;187:110324.

[13] Sanda A, Arriola I, Navas VG, Bengoetxea I, Gonzalo O. Ultrasonically assisted drilling of carbon fibre reinforcedplastics and Ti6Al4V. J Manuf Process 2016;22:169–76.

[14] Liu Y, Geng D, Shao Z, Zhou Z, Jiang X, Zhang D. A study on strengthening and machining integrated ultrasonic peening drilling of Ti-6Al-4V. Mater Des 2021;212:110238.

[15] Shokrani A, Al-Samarrai I, Newman ST. Hybrid cryogenic MQL for improving tool life in machining of Ti-6Al-4V titanium alloy. J Manuf Process 2019;43:229–43.

[16] Niketh S, Samuel GL. Surface texturing for tribology enhancement and its application on drill tool for the sustainable machining of titanium alloy. J Clean Prod 2018;167:253–70.

[17] Khanna N, Shah P, Chetan. Comparative analysis of dry, flood, MQL and cryogenic CO_2 techniques during the machining of 15–5-PH SS alloy. Tribol Int 2020;146:106196.

[18] Yildirim CV, Kivak T, Sarikaya M, Sirin S. Evaluation of tool wear, surface roughness/topograpgy and chip morphology when machining Ni-based alloy 625 under MQL, cryogenic cooling and cryo MQL. J Mater Res Technol 2020;9(2):2079–92.

[19] Gajarani KK. Assessment of cryo-MQL environment for machining of Ti-6Al-4V. J Manuf Process 2020;60:494–502.

[20] Agrawal C, Khanna N, Pruncu CI, Singla AK, Gupta MK. Tool wear progression and its effects on energy consumption and surface roughness in cryogenic assisted turning of Ti-6Al-4V. Int J Adv Manuf Technol 2020;111:1319–31.

[21] Agrawal C, Wadhwa J, Pitroda A, Pruncu CI, Sarikaya M, Khanna N. Comprehensive analysis of tool wear, tool life, surface roughness, costing and carbon emissions in turning Ti–6Al–4V titanium alloy: cryogenic versus wet machining. Tribol Int 2021;153:106597.

[22] Khanna N, Shah P, Lacalle LNLd, Rodriguez A, Pereira O. In pursuit of sustainable cuttingfluid strategy for machining Ti-6Al-4V using life cycle analysis. Sustain Mater Technol 2021;21:e00301.

[23] Kaynak Y, Gharibi A. Cryogenic machining of titanium Ti-5553 alloy. J Manuf Sci Eng 2019;141:041012.

[24] Jamil M, Zhao W, He N, Gupta MK, Sarikaya M, Khan AM, et al. Sustainable milling of Ti-6Al-4V: a trade-off between energy efficiency, carbon emissions and machining characteristics under MQL and cryogenic environment. J Clean Prod 2021;281:125374.

[25] Khanna N, Agrawal C, Gupta MK, Song Q, Singla AK. Sustainability and machinability improvement of Nimonic-90 using indigenously developed green hybrid machining technology. J Clean Prod 2020;263:121402.

[26] Agrawal C, Khanna N, Gupta MK, Kaynak Y. Sustainability assessment of in-house developed environment-friendly hybrid techniques for turning Ti-6Al-4V. Sustain Mater Technol 2020;26:e00220.

[27] Airao J, Nirala CK, Lacalle LNLd, Khanna N. Tool wear analysis during ultrasonic assisted turning of nimonic-90 under dry and wet conditions. Metals 2021;11(8):1253.

[28] Weinert K, Inasaki I, Sutherland JW, Wakabayashi T. Dry machining and minimum quantity lubrication. CIRP Ann - Manuf Technol 2004;53:511–37.

[29] Tapoglou N, Lopez MIA, Cook I, Taylor CM. Investigation of the influence of CO_2 cryogenic coolant application on tool wear. Proc CIRP 2017;63:745–9.

[30] Vipindas K, Mathew J. Wear behavior of TiAlN coated WC tool during micro end milling of Ti-6Al-4V and analysis of surface roughness. Wear 2019;424–425:165–82.

[31] Biksa A, Yamamoto K, Dosbaeva G, Veldhuis SC, Fox-Rabinovich GS, Elfizy A, et al. Wear behavior of adaptive nano-multi layered AlTiN/MexN PVD coatings during machining of aerospace alloys. Tribol Int 2010;43:1491–9.

[32] Çalışkan H, Küçükköse M. The effect of aCN/TiAlN coating on tool wear, cutting force, surface finish and chip morphology in face milling of Ti6Al4V superalloy. Int J Ref Mater Hard Met 2015;50:304–12.

[33] Stephenson DA, Agapiou JS. Metal cutting theory and practice. New York: CRC Press, MARCEL DEKKER, INC.; 1997.

[34] Kramer BM. On tool materials for high speed machining. J Eng Ind 1987;109:87–91.

[35] Pusavec F, Deshpande A, Yang S, M'Saoubi R, Kopac J, Dillon Jr OW, et al. Sustainable machining of high temperature Nickel alloy – inconel 718: Part 1 – predictive performance models. J Clean Prod 2014;81:255–69.

[36] Jayal AD, Balaji AK. Effects of cutting fluid application on tool wear in machining: interactions with tool-coatings and tool surface features. Wear 2009;267:1723–30.

[37] Sadik MI, Isakon S. The role of PVD coating and coolant nature in wear development and tool performance in cryogenic and wet milling of Ti-6Al-4V. Wear 2017;386–387:204–10.

[38] Wang CY, Xie YX, Qin Z, Lin HS, Yuan YH, Wang QM. Wear and breakage of TiAlN- and TiSiN-coated carbidetools during high-speed milling of hardened steel. Wear 2015;336–337:29–42.

[39] Stolf P, Paiva JM, Ahmed YS, Endrino JL, Goel S, Veldhuis SC. The role of high-pressure coolant in the wear characteristics of WC-Co tools during the cutting of Ti–6Al–4V. Wear 2019;440–441:203090.

[40] Lenart A, Pawlus P, Dzierwa A, Wos S, Reizer R. The effect of surface texture on lubricated fretting. Materials 2020;13(21):4886.

[41] Chetan, Behra BC, Ghosh S, Rao PV. Wear behavior of PVD TiN coated carbide inserts during machining of Nimonic 90 and Ti6Al4V superalloys under dry and MQL conditions. Ceram Int 2016;42:14873–85.

[42] Airao J, Nirala CK. Finite element modelling of ultrasonic assisted turning with external heating. Proc CIRP 2021;102:61–6.

[43] Khanna N, Airao J, Gupta MK, Song Q, Liu Z, Mia M, et al. Optimization of power consumption as-sociated with surface roughness in ultrasonic assisted turning of Nimonic-90 using hybrid particle swarm-simplex method. Materials 2019;12:3418.

[44] Pawlus P, Reizer R, Żelasko W. Two-process random textures: measurement, characterization, modeling and tribological impact: a review. Materials 2022;15(1):268.

[45] Pawlus P, Reizer R, Wieczorowski M. Analysis of surface texture of plateau-honed cylinder liner – a review. Prec Eng 2021;72:807–22.

[46] Zhang D, Shao Z, Geng D, Jiang X, Liu Y, Zhou Z, et al. Feasibility study of wave-motion milling of carbon fiber reinforced plastic holes. Int J Extrem Manuf 2021;3:01401.

[47] Kaynak Y, Karaca HE, Noebe RD, Jawahir IS. Tool-wear analysis in cryogenic machining of NiTi shape memory alloys: a comparison of tool-wear performance with dry and MQL machining. Wear 2013;306:51–63.

[48] Geng D, Liu Y, Shao Z, Zhang M, Jiang X, Zhang D. Delamination formation and suppression during rotary ultrasonic elliptical machining of CFRP. Comp Part B 2020;183:107698.

[49] Swirad S, Pawlus P. The influence of ball burnishing on friction in lubricated sliding. Materials 2020;13(21):5027.

[50] Airao J, Kishore H, Nirala CK. Tool wear behaviour in μ-turning of nimonic 90 under vegetable oil based cutting fluid. ASME J Micro Nano Manuf 2021;9(4):041003.

[51] Airao J, Nirala CK. Analytical modelling of machining forces and friction characteristics in ultrasonic assisted turning process. ASME J Manuf Sci Eng 2021;144:021014.

[52] Bermingham MJ, Kirsch J, Sun S, Palanisamy S, Dargusch MS. New observations on tool life, cutting forces and chip morphology in cryogenic machining Ti-6Al-4V. Int J Mach Tool Manuf 2011;51:500–11.